Evaluation of Imaging Windows for Tau PET Imaging Using ^{18}F-PI2620 in Cognitively Normal Individuals, Mild Cognitive Impairment, and Alzheimer's Disease Patients

Chanisa Chotipanich[1] ⓘ, Monchaya Nivorn[1], Anchisa Kunawudhi[1], Chetsadaporn Promteangtrong[1], Natphimol Boonkawin[1], and Attapon Jantarato[1]

Abstract

Background: The study aimed to evaluate the appropriate uptake-timing in cognitively normal individuals, mild cognitive impairment (MCI), and Alzheimer's disease (AD) patients, using ^{18}F-PI 2620 dynamic PET acquisition.

Methods: Thirty-four MCI patients, 6 AD patients, and 24 cognitively normal individuals were enrolled in this study. A dynamic ^{18}F-PI 2620 PET study was conducted at 30-75 minutes post-injection in these groups. Co-registration was applied between the dynamic acquisition PET and T1-weighted MRI to delineate various cortical regions. The standardized uptake value ratio (SUVR) was used for quantitative analysis. P-mod software with the Automated Anatomical Labeling (AAL)-merged atlas was employed to generate automatic volumes of interest for 11 brain regions.

Results: The curves in most brain regions presented an average SUVR stability at 30-40 minutes post-injection in each group. The appropriate uptake-timing interval of ^{18}F-PI 2620 was 30-75 minutes post injection for AD group and 30-40 minutes post injection for both cognitively normal individuals and MCI groups.

Conclusion: Short uptake time around 30-40 minutes post-injection would be more comfortable and convenient for all patients, especially in those with dementia who were unable to stay motionless for long periods of scanning time in the scanner.

Keywords

^{18}F-PI 2620, Alzheimer's disease, tau protein, PET neurology, PET dynamic acquisition, appropriate uptake-timing

Introduction

The aging population, which reflects advances in medical technology and longer life expectancy, has become a global problem. Alzheimer's disease (AD) is a common age-related neurodegenerative disease, and early diagnosis can help to delay disease progression and improve quality of life. While the mechanisms underlying neurodegeneration are not fully understood, the hallmarks of neurodegenerative diseases include beta amyloid (Aβ) plaques and neurofibrillary tangles (NFTs), made from hyperphosphorylated tau proteins. The positron emission tomography (PET) has been approved for the detection of tau protein retention.[1] This plaque aggregation can appear early during the disease progression and precedes the presentation of clinical symptoms. Furthermore, NFTs have been shown to be correlated with neurodegenerative symptoms and cognitive decline.[1-4]

In recent decades, several PET ligands that can bind to tau deposits have been developed, and a set of radiotracers has also been developed to study the deposition and accumulation of these proteins in the living human brain. For instance, the pharmacokinetics and pharmacodynamics of ^{11}C-PBB3,

[1] National Cyclotron and PET Centre, Chulabhorn Hospital, Bangkok, Thailand

Corresponding Author:
Chanisa Chotipanich, National Cyclotron and PET Centre, Chulabhorn Hospital, Chulabhorn Royal Academy, 906 Kamphaeng Phet 6 Rd, Talat Bang Khen, Lak Si, Bangkok 10210, Thailand.
Email: chanisa.cho@pccms.ac.th

^{18}F-THK5117,[18]F-THK5351, and ^{18}F-AV-1451 have been investigated in both preclinical and clinical studies.[5,6] Despite their intensive development for precise selective binding to tau protein deposition, these first-generation tau tracers still demonstrate the variation binding called "off-target," with the lack of selectivity for tau binding. The newly developed tau tracer,[18]F-PI-2620, binding to all types of tau deposits (3 R, 4 R, and 3R/4 R) in vitro and its effective binding (with a lower off-target binding) to tau, is considered as high potential tau binding tracer.[7,8]

While drawing attention to the clinical use of ^{18}F-PI2620 as a second generation of tau imaging radiotracer, there are evidently quite a few optimized acquisition protocols. The highly reliable and precise quantitative assessment and visualization afforded by PET examination demands the standardization of protocols.[9] We then need to find the appropriate time for PET acquisition of proper imaging in diagnosis. The appropriate uptake-timing is defined as the most stable period of radiotracer retention in the brain. Hence, this study aimed to define the post-injection stable period for a high accuracy protocol in cognitively normal individuals, mild cognitive impairment (MCI) and AD patients, using ^{18}F-PI 2620.

Materials and Methods

This study was approved by the Human Research Ethics Committee of Chulabhorn Research Institute. Written informed consent was obtained from all participants before the study.

Participants

Twenty cognitively normal individuals (6 men, 14 women; aged 56-71 years; mean age $\pm$ SD: 63.6 $\pm$ 5.09 years), 34 MCI patients (12 men, 22 women; aged 56-85 years; mean age $\pm$ SD: 66.71 $\pm$ 6.01 years), and 6 AD patients (3 men, 3 women; aged 56-74 years; mean age $\pm$ SD: 64 $\pm$ 7.01 years) were enrolled in this study. The cognitively normal individuals were verified by neurologists and neuropsychiatrists. No normal individuals had a history of psychological or neurological diseases, psychotropic drug use, or cancer within the last 5 years. They also had a score 24 -30 on the Montreal Cognitive Assessment (MoCA) Thai version. The AD participants were assessed and diagnosed by clinicians, using the National Institute on Aging-Alzheimer's Association criteria for probable AD. Magnetic resonance imaging (MRI) was performed in all participants.

Procedure

All participants underwent tau positron emission tomography with ^{18}F-PI2620, using a Siemens PET/CT Biograph Vision scanner in 3D mode.

^{18}F-PI2620 Imaging Procedure

Dynamic imaging was performed 30 minutes after the intravenous injection of 185 MBq (5 mCi) of ^{18}F-PI2620. Dynamic brain PET/CT images were obtained for 45 minutes and brain CT images were acquired for attenuation correction. Image acquisition parameters included matrix size = 440, zoom = 2, and an all-pass filter. Image reconstruction was performed in 9 frames, 5 minutes per frame, using the True X (point spread function reconstruction) plus Time of flight reconstruction with 8 iterations, 5 subsets. All iterative reconstruction images were used for quantitative analysis.

MRI Acquisition

T1-weighted MRI (T1MRI) was acquired for all participants using an Ingenia 3.0-T Philips MRI system. The parameters for the 3D T1MRI included: voxel size 0.43/0.43/1.20 mm, no overlapping; TR of 6.4 ms; TE of 3.0 ms, which reconstructed to 512 $\times$ 512 over a field of view of 220 $\times$ 200 mm.

Data and Statistical Analysis

Data processing and analysis of PET images were conducted using the P-mod Neuro tool (PMOD Technologies, Switzerland).[18]F-PI-2620 PET images were automatically co-registered within each individual, using an automatic voxel of interest (VOI) method. The PET images were then registered to the T1MRI from each subject. The T1-MRI images were used for the registration and delineation of the brain reference regions, with the data being standardized to the Montreal Neurological Institute (MNI) T1MRI template atlas. VOIs were automatically outlined on the normalized MRI based on the maximum probability following the Automated Anatomical Labeling (AAL)-merged atlas. Then, the standardized uptake value ratios (SUVR) of ^{18}F-PI 2620 were analyzed for various brain regions, using the cerebellum as a reference region. Eleventh regions were measured consisted of the hippocampus, inferior temporal lobe, lingual gyrus, middle temporal lobe, occipital lobe, parahippocampus, parietal lobe, posterior cingulate gyrus, precuneus, fusiform and white matter.

We determined the stability of retention from the average SUVR in each region. Frames 1 and 2 were defined as 30-40 minutes and continued consequently until frame 9, which was 70-75 minutes post-injection. The average SUVR of frames 1 and 2 (30-40 minutes post injection) was calculated and termed "baseline." Then, the acquiring SUVR from following time frame (frame 3-9) was included for average calculation. This new average SUVR was termed the "compared average SUVR." The baseline from frames 1-2 were then compared with the compared SUVR average from frames 1-3. A significant difference between the 2 average time intervals indicated a variation of the SUVR. We excluded frame 3 and only used the average taken from frames 1-2. This time interval with no significant difference between the 2 average time intervals was the stable period and used for quantitative study. However, if the average SUVR was not significantly different between the frames 1-2 and frames 1-3 averages, the baseline average SUVR for comparison would be changed to the average SUVR for frames 1-3. The compared SUVR was the average SUVR

Table 1. The Characteristics of Study Subjects.

	Healthy control	MCI	AD
Number	20	34	6
Age, years, mean $\pm$ SD (range)	63.6 $\pm$ 5.09 (56-71)	66.71 $\pm$ 6.01 (56-85)	64 $\pm$ 7.01 (56-74)
Sex, number (%)			
Male	6 (30%)	12 (35%)	3 (50%)
Female	14 (70%)	22 (65%)	3 (50%)
Montreal Cognitive Assessment (MOCA) score	26.45 $\pm$ 1.90	21.81 $\pm$ 2.42	14.83 $\pm$ 5.6

Table 2. The P-Value at 95% Confidence Intervals from the Compared Average SUVR and Baseline Average SUVR in Cognitively Normal Individuals.

Brain regions	Baseline average SUVR time frame	Compared average SUVR time frame	P-value
Fusiform	Avg1-2	Avg1-3	0.0214
Hippocampus	Avg1-6	Avg1-7	0.0075
Inferior temporal	Avg1-4	Avg1-5	0.0155
Lingual	Avg1-2	Avg1-3	0.0009
Middle temporal	Avg1-4	Avg1-5	0.0099
Occipital	Avg1-2	Avg1-3	0.0002
Parahippocampus	Avg1-8	Avg1-9	0.66
Parietal	Avg1-2	Avg1-3	0.0273
Posterior cingulate	Avg1-2	Avg1-3	0.0345
Precuneus	Avg1-2	Avg1-3	0.0334
White matter	Avg1-4	Avg1-5	0.0462

from frames 1 to 4. This process was continued until the baseline average SUVR frames 1-8 to compare with the compared average SUVR frames 1-9.

STATA software version 11 (Stata Corp, USA) was applied for all analyses. Shapiro-Wilk W-test was employed to assess normal distribution. A normal distribution of SUVR at each time point was indicated by p-value ≤ 0.05. SUVR with normally distributed was compared using paired t-tests. Intervals without normally distributed were compared using Wilcoxon signed-rank tests for non-parametric data.

Results

The demographic characteristics of the study subjects were shown in Table 1.
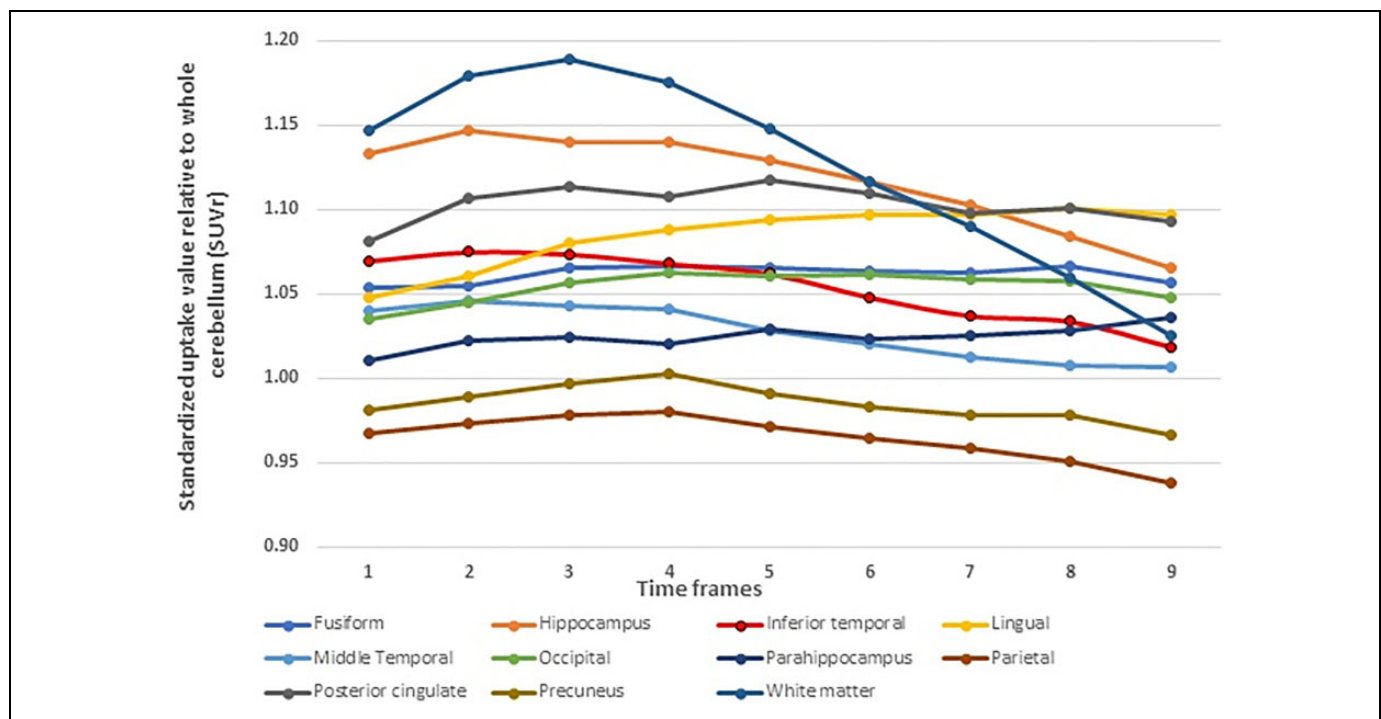
Figure 1. Average SUVR over time for each region in cognitively normal individuals.

Cognitively Normal Individuals

The greatest SUVR stability was demonstrated at the early phase of acquisition at frames 1-2 (30-40 minutes post injection). Regions showing SUVR average stabilities in the early phase included the fusiform, lingual, occipital, parietal posterior cingulate. Whist, precuneus, inferior temporal, middle temporal, and white matter, held the stable time at frames 1-4. In the remaining regions, accumulation of PI2620 remained stable until the later acquisition time of around frames 6. The parahippocampus exhibited a stable retention of PI2620 throughout the entire time period. The results were shown in Table 2 and Figure 1.

Table 3. The P-Value at 95% Confidence Intervals From the Compared Average SUVR and Baseline Average SUVR in MCI Groups.

| Brain regions	Baseline average SUVR time frame	Compared avg SUVR time frame	P-value
Fusiform	Avg1-3	Avg1-4	0.0212
Hippocampus	Avg1-4	Avg1-5	0.0025
Inferior temporal	Avg1-3	Avg1-4	0.0007
Lingual	Avg1-2	Avg1-3	0.0000
Middle temporal	Avg1-2	Avg1-3	0.0239
Occipital	Avg1-2	Avg1-3	0.0000
Parahippocampus	Avg1-3	Avg1-4	0.0318
Parietal	Avg1-4	Avg1-5	0.0024
Posterior cingulate	Avg1-2	Avg1-3	0.0087
Precuneus	Avg1-7	Avg1-8	0.0040
White matter	Avg1-3	Avg1-4	0.0017

MCI

There was a significant difference time interval between baseline and the average SUVR for frames 1-2 and the average SUVR for frames 1-3 (p-values 0.0212), including lingual gyrus, middle temporal lobe, occipital lobe, and posterior cingulate gyrus. The stabilities of SUVR for most regions were average of frames 1-2, corresponding to an uptake time of 30-40 minutes post-injection. The remaining with various results indicating different stable time intervals for each region included hippocampus and parietal. The SUVR stabilities over time frames for hippocampus and parietal lobe were from frames 1-4. Inferior temporal and white matter were shown stabilities at frames 1 to 3, while the stability in precuneus was maintained from frames 1-7. The results were shown in Table 3 and Figure 2.

AD

Interestingly, all regions in the AD group demonstrated average SUVR stability from frame 1 to frame 9. There was no significant change in the average SUVR over time, except for white matter, in which stability was found until frame 7. The results were shown in Table 4 and Figure 3.

From the 3 groups, we found that the cognitively normal individuals and MCI patients demonstrated a stable SUVR average in most regions at around 30-40 minutes post-injection. While, the average SUVR in the AD group was stable throughout the whole examination, of frames 1-9, at 30-75 minutes post-injection. The results were shown in Figure 4.
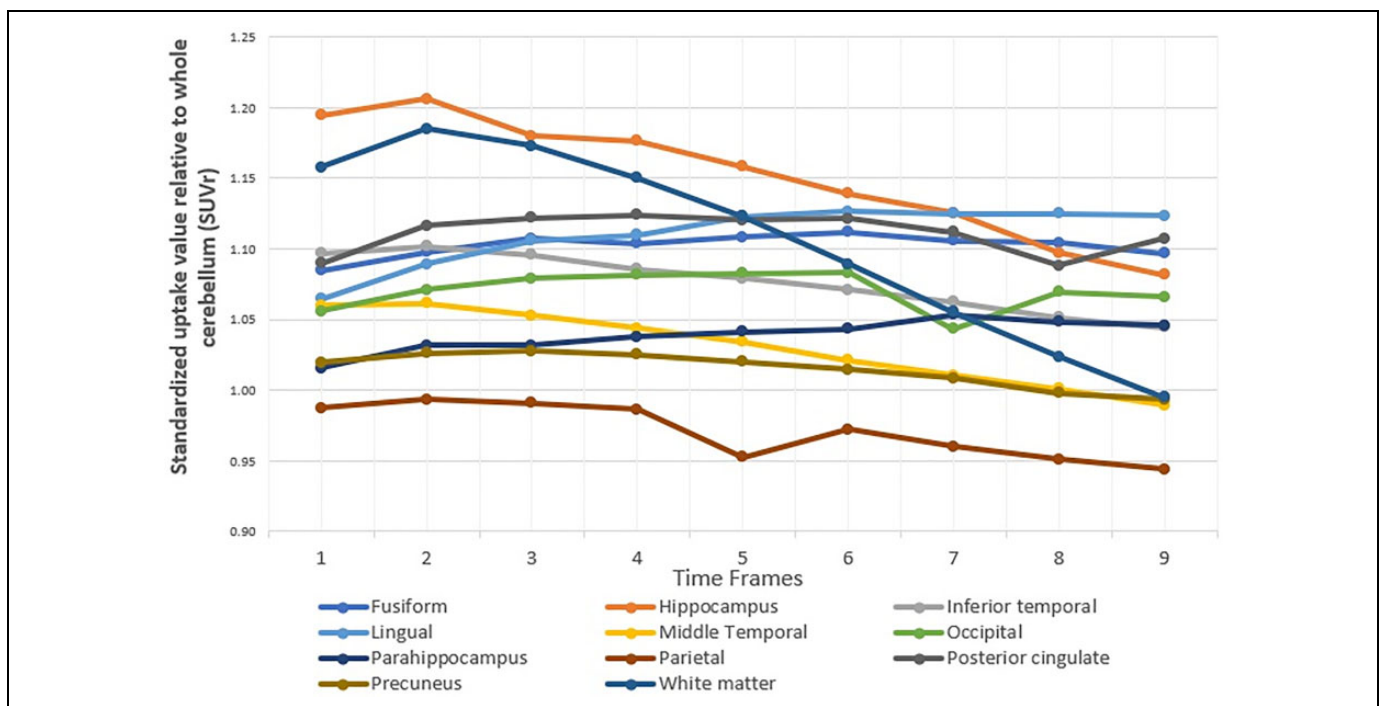
Figure 2. Average SUVR over time for each region in MCI groups.

The raw data of tendency of SUVR over time frames in each patient of cognitively normal individuals, MCI and AD groups are shown in supplementary file 1-3, respectively. Figure 5 shows PI2620 PET brain images of patients with AD, MCI and cognitively normal individual.

Discussion

PI2620 has been studied in clinical trials and recognized as the second-generation compound for reliable results on tau protein deposition in different brain regions.[1] The average SUVR in the 3 groups have strong implications for the clinical evaluation and differentiation of AD from MCI and cognitively normal individuals diagnoses.

Table 4. The P-Value at 95% Confidence Intervals From the Compared Average SUVR and Baseline Average SUVR in AD Groups.

Brain regions	Baseline average SUVR time frame	Compared avg SUVR time frame	P-value
Fusiform	Avg1-8	Avg1-9	0.34
Hippocampus	Avg1-8	Avg1-9	0.16
Inferior temporal	Avg1-8	Avg1-9	0.61
Lingual	Avg1-8	Avg1-9	0.46
Middle temporal	Avg1-8	Avg1-9	0.9165
Occipital	Avg1-8	Avg1-9	0.3824
Parahippocampus	Avg1-8	Avg1-9	0.7532
Parietal	Avg1-8	Avg1-9	0.1159
Posterior cingulate	Avg1-8	Avg1-9	0.8814
Precuneus	Avg1-8	Avg1-9	0.2489
White matter	Avg1-7	Avg1-8	0.0032

In our study, the AD group not only showed an elevated level of tau protein deposition, but also a prolonged high average SUVR over time frames 1 to 9 in all brain regions. Additionally, the all brain regions revealed average SUVR values over 1.25, especially in significant brain areas of the inferior temporal lobes, precuneus, posterior cingulate gyrus, and occipital lobe, associated with tau deposition in AD.[10-14] Our findings also corroborated those of Stephens et al.,[15] Villemagne et al.,[16] Mormino et al.[17] and Muller et al,[18] who described similar results on the ability of this novel tau radiotracer to bind to tau protein in AD brain. While, the average SUVR of the cognitively normal individuals and MCI groups was similar average SUVR over time frames, but higher SUVR in all time frames at most regions of the AD group. As in previous reports, a correlation was found between tau radiotracers with cognition in preclinical AD.[19]

Moreover, both quantitative and qualitative neuro-analysis of PET required a great accuracy for time point. From our study, the appropriate uptake-timing for average SUVR was 30-40 minutes post injection in cognitively normal individuals and MCI. It was emphasized that selection of an inappropriate time interval for the imaging analysis could affect the diagnostic results. For instance, if we only analyzed the later phase at around 40 minutes post-injection, images may have low signal intensity due to rapid wash out and the quantitative average SUVR may be underestimated due to the wash-out process. Interestingly, the stable SUVR over time frames in the AD group indicated that the time interval used for the analysis may have only a subtle effect on the results in the AD group. That means, the average SUVR was stable from 30-75 minutes post injection in the AD group.
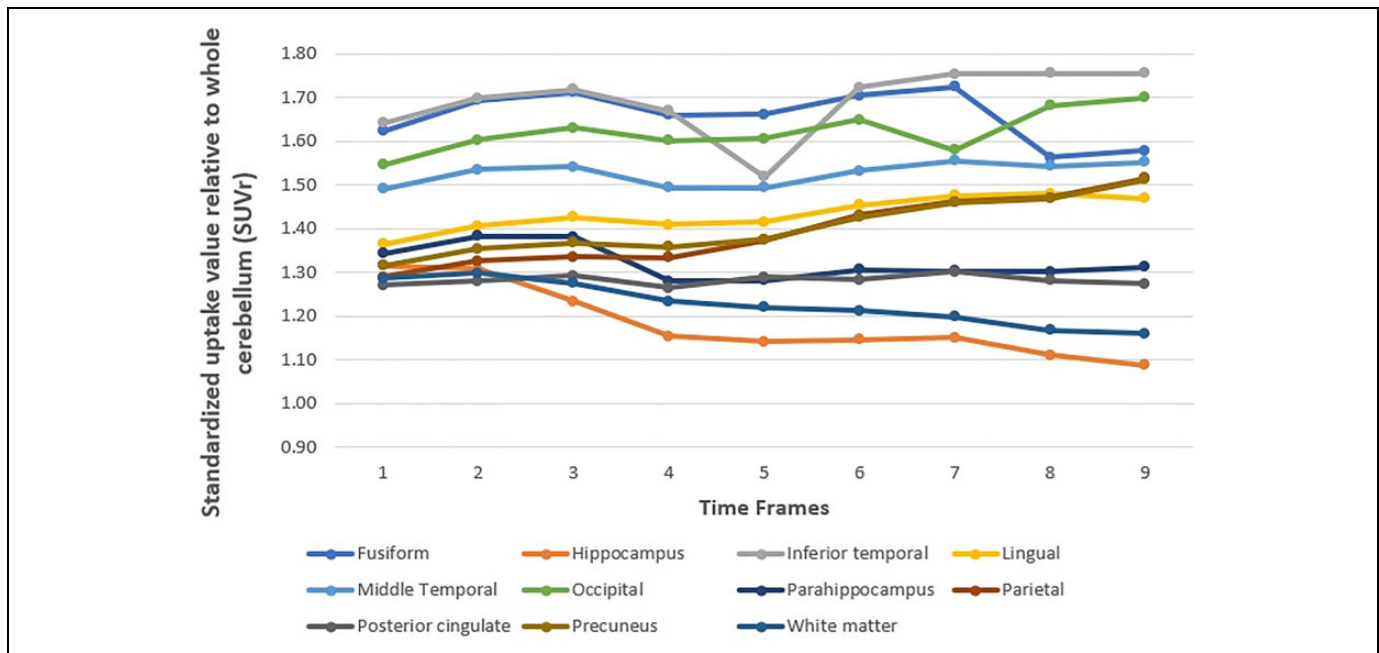
Figure 3. Average SUVR over time for each region in AD groups.
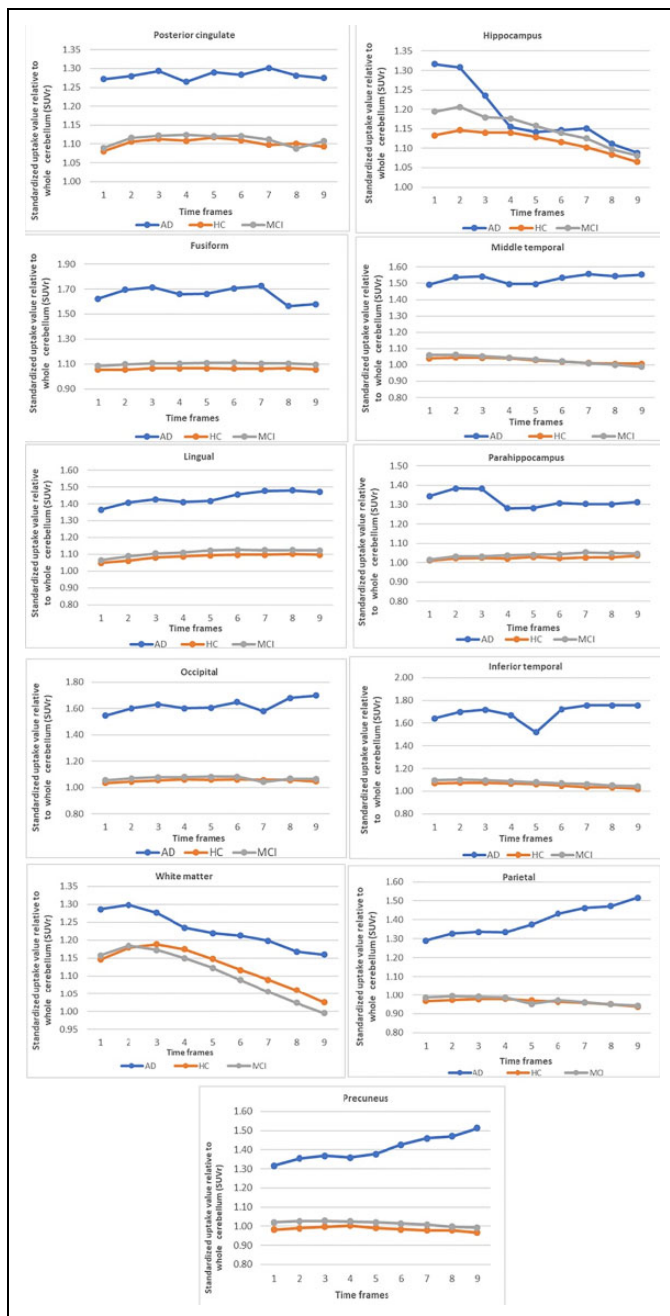
**Figure 4.** Average SUVR over time for 11 regions in cognitively normal individuals, MCI and AD groups.

Our appropriate uptake-timing could be described by 2 reasons. First, it was from the stable average SUVR in the inferior temporal gyrus calculated from the compared average SUVR between 30-35 minutes post-injection and average SUVR 30-40 post injection. Second, the SUVR curve was shown the PI2620 accumulation in most brain regions before 40 minutes post-injection. The wash out began after 40 minutes post injection. However, there were different patterns in each group. Given that the stability of uptake time in most regions of the AD group was longer than MCI and cognitively normal individuals groups, the appropriate uptake-timing for AD group

analysis could be then extended to 40-75 minutes post-injection. This stability could be explained by the prolonged binding of PI2620 with phosphorylated tau in the AD brain.[15] Furthermore, the PI2620 excretion occurred rapidly in the brain with less tau deposition, including the cognitively normal individuals and MCI subjects, with a similar uptake time pattern in this study

Previous studies revealed some discordances about the analysis timing for PI2620. Stephen et al.[15] performed a dynamic acquisition from 0 to180 minutes post-injection and reported that a stable accumulation of PI2620 was obtained 60-90 minutes post-injection. According to the plateaus of their SUVR time curves, Barret et al.[20] selected an optimal time of 90-100 minutes post injection for the AD group and 60-70 minutes for the healthy control group. Mormino et al.[17] used the uptake at 60-90 minutes for SUVR analysis. In accordance with Villemagne et al.,[16] it showed tracer-reversible kinetics and an apparent steady state at 80-90 minutes after PI2620 injection. Muller et al.[18] examined the quantification of PI2620 in brain regions using DVR and SUVR for 30 minutes imaging windows between 30-90 minutes, providing outstanding and significant discrimination between AD and healthy control subjects. Moreover, the findings from Bullich et al.[21] defined PI2620 PET acquisition time between 45-75 minutes post injection, with great accuracy for quantification analysis. Nevertheless, the SUVR calculation of those previous studies employed the very late time post-injection in comparison with our findings. As Barret et al.'s results,[20] there was an early equilibrium of PI2620 accumulation in cognitively normal individuals and prolonged uptake in the AD. The disagreement of optimized time analysis may be due to different method analysis or the conditions of each individual, such as brain clearance in various ethnics.

Noticeably, previous studies found the equilibrium time of PI2620 accumulation focused on complex analysis, including time activity curves (TACs) or SUV over time with long dynamic acquisition from 0 to 180 minutes post injection.[18] Conversely, the methodology in our study was adapted for application in actual practice. Firstly, the reduction of the acquisition protocol from previous studies which acquired the data 180 minutes (from 0 to 180 minutes post injection)[15,17] to about 45 minutes (30-75 minutes post injection) as suitable time for AD patients or incorporated subjects. Secondly, the SUVR calculated from cerebellum normalization uptake was selected for appropriate uptake time analysis, instead of SUV or TACs since we used the SUVR in routine clinical practice for AD diagnosis and PET interpretation based on SUVR average over time frame.[18-24] Hence, the average SUVR stability was assumed to be more reliable and appropriate in the routine practical analysis.

Finally, our results could have practical implications for defining the acquisition protocol in clinical practice in most PET centers, using PI2620 in shorter uptake time at around 30-40 minutes post-injection. This shorter appropriate uptake-timing would be more comfortable and convenient for patients, especially in those with dementia who were unable to
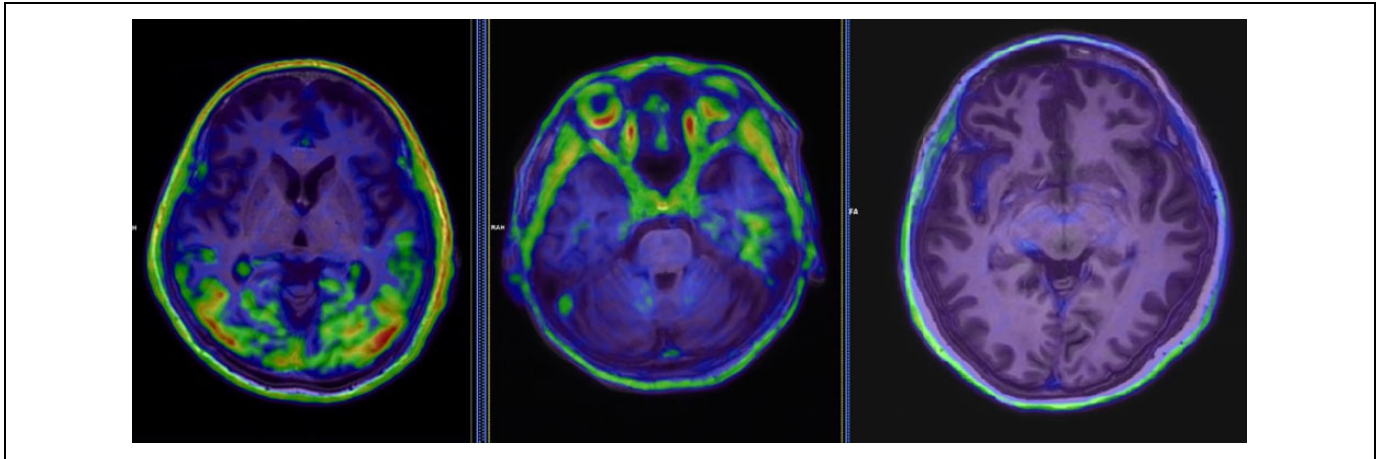
Figure 5. Left: A 59-year-old male AD patient with MoCA score 19. Fused 18F-PI-2620 PET /T1-weighted MRI image shows increased 18F-PI-2620 uptake at inferior temporal, occipital and parietal cortices. Middle: A 75-year-old male MCI patient with MoCA score 23. Fused 18F-PI-2620 PET /T1-weighted MRI image shows increased 18F-PI-2620 uptake at mesial temporal and inferior temporal cortices. Right: A 63-year-old cognitively normal female with MoCA score 29. Fused 18F-PI-2620 PET /T1-weighted MRI image shows no abnormal 18F-PI-2620 uptake at neocortical regions.

stay motionless for long periods of scanning time in the scanner. Moreover, if the present findings could be replicated with reliable and consistent results and informed an effective protocol for quantitative and qualitative analysis, a dynamic study with very long acquisition and complicated reconstruction may be adapted to the static acquisition just only from 10 minutes to 30-40-minute post-injection. This short data acquisition period would bring further time and cost efficiency, with less exposure to radiation for staffs, and lowest resource scanner usage.

Limitations

Our study was limited by the small number of participants, which might have decreased the statistical power and may interfere with the average SUVR, resulting to the variation of SUVR in some time points. We did not specify the type of MCI for each patient in this study, however we applied the Clinical Dementia Rating (CDR) scale for MCI diagnosis. The lower value and significant decreasing of SUVR in some AD subjects could be from unintended patient movement in later time frames due to the AD symptom and the technical aspect from the SUVR calculated using P-mod software which might be subject to variation in some subjects with noticeable brain atrophy, because of the lack of a voxel-based morphology correction. As a result, the visual analysis may not directly describe uptake tendency in this group. However, the statistical analysis demonstrated the stability of average SUVR over 9 frames time in the AD group. Furthermore, we did not perform the PET dynamic acquisition from 0 to 75 minutes and distribution volume ratio (DVR) calculation due to various complexities in the process for protocol setting and blood samplings. Then, from our setting protocol, it was possible that we missed the maximum uptake in some brain regions and did not directly determine the maximum uptake. However, the starting point of acquisition at 30 minutes post-injection should still be preferable due to the acquisition of relative peak accumulation in significant brain regions. Thus, the conclusion from average SUVR could be enough for PI2620 appropriate uptake-timing. However, the suggested protocol could be adapted according to the scanner performance due to the detector sensitivity and reconstruction method.

Conclusion

The ^{18}F-PI-2620 is a novel radiotracer with potential applications for the clinical diagnosis of tau protein deposition. Our findings describe the appropriate uptake-timing of PI2620 in cognitively normal individuals, MCI, and AD patients. Short uptake time around 30-40 minutes post-injection would be more comfortable and convenient for all patients. The results could be helpful in clinical practice for the development of a standardized study protocol that grants accurate quantitative and qualitative results.

ORCID iD

Chanisa Chotipanich https://orcid.org/0000-0002-0041-4938

Supplemental Material

Supplemental material for this article is available online.

References

1. Leuzy A, Chiotis K, Lemoine L, et al. Tau PET imaging in neurodegenerative tauopathies—still a challenge. *Mol Psychiatr*. 2019;24(8):1112–1134.

2. Crous-Bou M, Minguillón C, Gramunt N, Molinuevo JL. Alzheimer's disease prevention: from risk factors to early intervention. *Alzheimers Res Ther*. 2017;9(1):71.

3. Weller J, Budson A. Current understanding of Alzheimer's disease diagnosis and treatment. *F1000Res*. 2018 Jul 31;7. Accessed October 6, 2019. https://www.ncbi.nlm.nih.gov/pmc/articles/PMC6073093/

4. Christensen K, Doblhammer G, Rau R, Vaupel JW. Ageing populations: the challenges ahead. *Lancet*. 2009;374(9696): 1196–1208.

5. Kroth H, Oden F, Molette J, et al. Discovery and preclinical characterization of [18F] PI-2620, a next-generation tau PET tracer for the assessment of tau pathology in Alzheimer's disease and other tauopathies. *Eur J Nucl Med Mol Imaging*. 2019;46(10): 2178–2189.

6. Okamura N, Harada R, Ishiki A, Kikuchi A, Nakamura T, Kudo Y. The development and validation of tau PET tracers: current status and future directions. *Clin Transl Imaging*. 2018;6(4): 305–316.

7. Wang YT, Edison P. Tau imaging in neurodegenerative diseases using positron emission tomography. *Curr Neurol Neurosci Rep*. 2019;19(7):45.

8. Leuzy A, Chiotis K, Lemoine L, et al. Tau PET imaging in neurodegenerative tauopathies—still a challenge. *Mol Psychiatr*. 2019;24(8):1112–1134.

9. Schmidt ME, Chiao P, Klein G, et al. The influence of biological and technical factors on quantitative analysis of amyloid PET: points to consider and recommendations for controlling variability in longitudinal data. *Alzheimers Dement*. 2015;11(9): 1050–1068.

10. Brier MR, Gordon B, Friedrichsen K, et al. Tau and Abeta imaging, CSF measures, and cognition in Alzheimer's disease. *Sci Transl Med*. 2016;8(338):338–366.

11. Ishiki A, Okamura N, Furukawa K, et al. Longitudinal assessment of tau pathology in patients with Alzheimer's disease using [18F] THK-5117 positron emission tomography. *Plos One*. 2015; 10(10):e0140311.

12. Johnson KA, Schultz A, Betensky RA, et al. Tau positron emission tomographic imaging in aging and early Alzheimer disease. *Ann Neurol*. 2016;79(1):110–119.

13. Ossenkoppele R, Schonhaut DR, Schöll M, et al. Tau PET patterns mirror clinical and neuroanatomical variability in Alzheimer's disease. *Brain*. 2016;139(Pt 5):1551–1567.

14. Schwarz AJ, Yu P, Miller BB, et al. Regional profiles of the candidate tau PET ligand 18F-AV-1451 recapitulate key features of Braak histopathological stages. *Brain*. 2016;139(Pt 5): 1539–1550.

15. Stephens A, Seibyl J, Mueller A, et al. Clinical update: 18f-Pi-2620, a next generation tau pet agent evaluated in subjects with Alzheimer's disease and progressive supranuclear palsy. *Alzheimer Dement*. 2018;14(7):179. doi:10.1016/j.jalz.2018.06. 2287

16. Villemagne V, Dore V, Mulligan R, et al. Evaluation of 18F-PI-2620, a second-generation selective tau tracer for the assessment of Alzheimer's and non-Alzheimer's tauopathies. *J Nucl Med*. 2018;59(suppl 1):410–410.

17. Mormino EC, Nadiadwala A, Azevedo C, et al. Tau pet imaging with 18f-Pi2620 in aging and Alzheimer's disease. *Alzheimer Dement*. 2018;14(7):1577–1578. doi:10.1016/j.jalz. 2018.07.138

18. Mueller A, Bullich S, Barret O, et al. Tau PET imaging with 18F-PI-2620 in patients with Alzheimer's disease and healthy controls: a first-in-human study. *J Nucl Med*. 2020;61(6): 911–919.

19. Hanseeuw BJ, Betensky RA, Jacobs HIL, et al. Association of amyloid and tau with cognition in preclinical Alzheimer disease: a longitudinal study. *JAMA Neurol*. 2019;76(8):915–924.

20. Barret O, Seibyl J, Stephens A, et al. Initial clinical pet studies with the novel tau agent 18-F Pi-2620 in Alzheimer's disease and controls. *J Nucl Med*. 2017;58(suppl 1):630–630.

21. Bullich S, Barret O, Constantinescu C, et al. Evaluation of dosimetry, quantitative methods and test-retest variability of 18F-PI-2620 PET for the assessment of tau deposits in the human brain. *J Nucl Med*. 2019;61(6):920–927.

22. Hanseeuw BJ, Betensky RA, Jacobs HIL, et al. Association of amyloid and tau with cognition in preclinical Alzheimer disease: a longitudinal study. *JAMA Neurol*. 2019;76(8):915–924.

23. Lockhart SN, Baker SL, Okamura N, et al. Dynamic PET measures of tau accumulation in cognitively normal older adults and Alzheimer's disease patients measured using [18F] THK-5351. *Plos One*. 2016;11(6):e0158460.

24. Vemuri P, Lowe VJ, Knopman DS, et al. Tau-PET uptake: regional variation in average SUVR and impact of amyloid deposition. *Alzheimers Dement*. 2017;6:21–30.